Journal of Catalysis 285 (2012) 235–241

Contents lists available at SciVerse ScienceDirect

Journal of Catalysis

journal homepage: www.elsevier.com/locate/jcat

Active species of copper chromite catalyst in C–O hydrogenolysis of 5-methylfurfuryl alcohol

Keenan L. Deutsch, Brent H. Shanks *

Department of Chemical and Biological Engineering, Iowa State University, Ames, IA 50011, USA

ARTICLE INFO

Article history:
Received 12 July 2011
Revised 7 September 2011
Accepted 24 September 2011
Available online 8 November 2011

Keywords:
Hydrogenolysis
Copper catalyst
Copper chromite
5-Hydroxymethylfurfural
2,5-Dimethylfuran
Deoxygenation
Biorenewables

ABSTRACT

The active sites of copper chromite catalyst, $CuCr_2O_4{\cdot}CuO$, were investigated for the condensed-phase hydrogenolysis of 5-methylfurfuryl alcohol to 2,5-dimethylfuran at 220 °C. The bulk and surface features of the catalyst were characterized by XRD, H_2-TPR, N_2 adsorption, CO chemisorption, N_2O titration, NH_3-TPD, XPS, and AES. Maxima of both of the potential active species, Cu^0 and Cu^+, occurred after reduction in H_2 at 300 °C compared to 240 and 360 °C. These Cu^0 and Cu^+ maxima also coincided with the highest specific rate of reaction based on the surface area of the reduced catalyst. The trends of Cu^0 and Cu^+ observed by N_2O titration and CO chemisorption were also observed qualitatively by AES. Correlations between activity and the possible active species suggested that Cu^0 was primarily responsible for the activity of the catalysts.

1. Introduction

There are many technical and economic challenges facing the production of biorenewable chemicals and fuels. One of these challenges is the high oxygen content of biorenewable feedstocks and the intermediates derived through catalytic or pyrolytic conversions. Hydrogenolysis of C–O bonds is a class of reaction that is likely to play an important role in the processing of biorenewables. Furfural and 5-hydroxymethylfurfural (HMF) are intermediates that can be formed by the acid-catalyzed dehydration of C_5 and C_6 carbohydrates and in the pyrolysis of biomass [1–6]. Recently, the Dumesic group has explored deoxygenation via hydrogenolysis of HMF to form 2,5-dimethylfuran (DMF), which has favorable fuel characteristics relative to ethanol [2].

Considerable literature exists on the hydrogenation of furfural to furfuryl alcohol, in which 2-methylfuran is produced as a byproduct of a consecutive hydrogenolysis reaction [6–17]. Literature focusing on C–O hydrogenolysis of furfural and HMF is limited and encompasses numerous screening studies of copper-containing catalysts, which show that copper can be used to perform this transformation at high yields [2,8,18–23]. Copper catalysts have been shown to preferentially cleave C–O bonds without significant C–C cleavage or hydrogenation of the furan ring. The development of catalysts that can perform C–O hydrogenolysis without excessive hydrogen consumption may be important in the deoxygenation of renewable feedstocks containing significant amounts of furanic and phenolic species [24–26]. Furthermore, many of these phenolic and carbohydrate-derived compounds are not very volatile, such as HMF (b.p. 291 °C), and may be more amenable to condensed-phase processing than to conventional vapor-phase processing.

The active species of copper catalysts has been the center of debate for many years in the methanol synthesis literature [27]. In simplified terms, part of this discussion has centered on the role of metallic copper as the primary active species or the potential role of a Cu^+ species as an active component [27]. Aspects of this active site discussion have also been invoked in relation to other hydrogenation reactions such as the hydrogenation of furfural to furfuryl alcohol. The Vannice group has claimed that both Cu^0 and a Cu^+ species play a role in the catalytic cycle and are necessary for optimal performance [12,13]. However, little work has been done to characterize and understand the sites involved in C–O hydrogenolysis of furanic and phenolic compounds that contain α-unsaturated bonds.

Copper chromite, $CuCr_2O_4{\cdot}CuO$, is a conventional catalyst that has been used industrially to convert furfural to furfuryl alcohol, and it can also effectively perform C–O hydrogenolysis of furfural and HMF [2,13,28]. The focus of this work is on examining the relationship of the Cu^0 and Cu^+ surface concentrations of a copper chromite catalyst to its activity in a simplified reaction system. The simplified system only involves the C–O hydrogenolysis of 5-methylfurfuryl alcohol to DMF in a *tert*-amyl alcohol solvent

* Corresponding author.
E-mail address: bshanks@iastate.edu (B.H. Shanks).

0021-9517/$ - see front matter © 2011 Elsevier Inc. All rights reserved.
doi:10.1016/j.jcat.2011.09.030

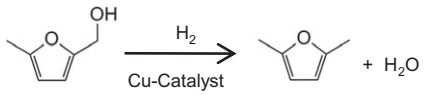

Scheme 1. Catalytic conversion of 5-methylfurfuryl alcohol to DMF.

rather than examining the conversion all the way from HMF. 5-Methylfurfuryl alcohol was chosen as the reactant because it is an intermediate in the hydrogenolysis of HMF to DMF as shown in Scheme 1.

In this work, the catalyst was characterized with N_2 adsorption, temperature-programmed reduction (TPR), N_2O titration for quantification of Cu^0 sites, CO chemisorption for quantification of Cu^+ sites, X-ray diffraction (XRD), ammonia temperature-programmed desorption (NH_3-TPD), X-ray photoelectron spectroscopy (XPS), and Auger electron spectroscopy (AES) for the semi-quantitative determination of Cu^0:Cu^+. The relevance of surface species to the catalytic cycle can be determined by correlating the surface concentrations of catalyst species with initial rates of reaction.

2. Materials and methods

2.1. X-ray diffraction

X-ray diffraction (XRD) was performed using a Siemens D 500 diffractometer with a diffracted-beam monochromator tuned to Cu Kα radiation. The catalyst samples were prepared by reduction within a quartz tube placed in the heating zone of a tube furnace. They were reduced in 1 L/min H_2 (Linweld 99.995%) using a ramp rate of 2 °C/min to 240, 300, or 360 °C and were held at the final temperature for 1 h. Once cooled to room temperature under H_2 flow, the sample was passivated with flowing 1% O_2 in N_2 by diluting air with N_2 (Praxair 99.995%) at 1 L/min for 1 h.

2.2. Temperature-programmed reduction

Temperature-programmed reduction (H_2-TPR) of the copper chromite catalyst was performed using a Micromeritics AutoChem II 2920 equipped with a thermal conductivity detector (TCD). A reducing gas of 10% H_2 in Ar (Linweld certified) was used with a 5 °C/min ramp rate. A cold trap was used to condense water generated from the reduction, and the TCD observed the consumption of H_2.

2.3. N_2-adsorption BET method

N_2 adsorption was performed following the BET method on a Micromeritics ASAP 2020 to determine the total surface area of the untreated copper chromite catalyst, and the copper chromite catalysts reduced ex situ and passivated following the same reduction and passivation procedure discussed in Section 2.1.

2.4. CO chemisorption

Irreversible CO adsorption isotherms were used to quantify the amount of surface Cu^+ as described by Rao et al. [12,13]. The isotherms were collected with a chemisorption module of the Micromeritics ASAP 2020 instrument. Catalysts were reduced in situ with H_2 (Linweld 99.995%) at 240, 300, and 360 °C for 1 h using a 10 °C/min ramp. Samples were then cooled to 35 °C, and a total adsorption isotherm was collected using 50–500 mm Hg CO (Matheson Purity). The sample tube was then evacuated for 30 min, and the measurement was repeated to determine the reversible adsorption isotherm. The difference between the total and reversible was used to determine the irreversible isotherm. The irreversible adsorption was the asymptotic value obtained by averaging the irreversible isotherm points between 150 and 500 mm Hg CO. Since the molecular area of the Cu^+ adsorption site is not definitively known, the metallic Cu^0 atomic area of 0.068 nm^2/atom was used to estimate the surface area of Cu^+.

2.5. N_2O titration

The Cu^0 surface area was determined using N_2O titration, in which a stoichiometry of $2Cu^0$:$1N_2O$ corresponding to the reaction $2Cu^0 + N_2O(g) \rightarrow Cu_2O + N_2(g)$ and an atomic area of 0.068 nm^2/atom were used [29–31]. Samples were analyzed in a CE Instruments TPDRO-100 fixed bed reactor connected to a Pfeiffer QMS Thermostar mass spectrometer at the Fritz Haber Institute in Berlin, Germany. Samples were reduced in 5% H_2 in Ar using a ramp rate of 2 °C/min to 240, 300, and 360 °C. The reactor was cooled to 50 °C and then backfilled with Ar. Analysis was performed at 40 °C by flowing 97% N_2O over the reduced catalyst and observing the corresponding drop in N_2O concentration and increase in N_2 concentration on the mass spectrometer. The time interval of oxidation was used to determine the amount of N_2O consumed.

2.6. X-ray photoelectron spectroscopy and Auger electron spectroscopy

Samples were prepared by ex situ reduction in a tube furnace using H_2 (Linweld 99.995%) following the same temperature programs described in Section 2.1. Samples were cooled to room temperature under H_2 flow and purged with 1 L/min Ar for 30 min. The quartz tube was then sealed and loaded into a glove box with <1 ppm O_2, where the samples were removed and prepared for analysis to prevent oxidation upon exposure to air. X-ray photoelectron spectroscopy (XPS) and X-ray-induced Auger electron spectroscopy (AES) measurements were carried out on a Physical Electronics 5500 multitechnique system with a Mg source. Samples were mounted on double-sided tape with a measurement area of approximately 1 mm^2. Sample charging was experienced due to the presence of unreduced metal oxide. The characteristic satellite peak associated with the Cu^{2+} at a binding energy (BE) of 942 eV was not observed. Therefore, the data could be corrected for charging by setting the overlapping Cu^+/Cu^0 XPS peaks to 932.8 eV. AES was used to determine the relative ratios of Cu^+ and Cu^0 by deconvoluting and integrating the two peaks at 916.0 and 918.3 eV and taking the ratio of the respective areas. Data analysis was performed using CasaXPS software utilizing background subtraction and peak-shape fitting of standards.

2.7. Ammonia temperature-programmed desorption

Ammonia temperature-programmed desorption (NH_3-TPD) was performed with the Micromeritics AutoChem II 2920 by reducing the sample for 1 h in 10% H_2 in Ar at ramp rates of 2.8, 2.6, and 2.4 °C/min to final temperatures of 240, 300, and 360 °C, respectively. Samples were cooled to 240 °C and held for 30 min to allow H_2 desorption in Ar. Samples were then cooled to 50 °C and exposed to 9.9969% NH_3 in He (Matheson Tri-Gas) for 30 min. TPD was then performed up to a final temperature of 700 °C at a ramp rate of 10 °C/min.

2.8. Reaction testing

The materials used in the reaction system included a commercial copper chromite catalyst (Acros Organics), H_2 gas (Linweld 99.995%), and 5-methylfurfuryl alcohol (5-methyl-2-furanmethanol Acros Organics 97%) as the reactants and *tert*-amyl alcohol (Fisher Scientific, reagent grade) as the solvent. The catalyst was crushed and sieved to 53–75 μm and 106–150 μm, and both

samples were used in reaction testing to ensure the absence of internal mass transfer effects. The absence of external limitations on the mass transfer of the reactants from the bulk liquid to the catalyst surface and on hydrogen transfer from the gas to the liquid phase was confirmed by performing reaction tests at varying stirring rates and various catalyst loadings. Reactions were performed in an Autoclave Engineers 100-mL EZE batch reactor at 220 °C, 500 psi H_2, 500 rpm, and an initial concentration of 25 mM 5-methylfurfuryl alcohol. Five samples were taken at equal increments over 40 min, with the first sample taken at the start of the reaction (T = 220 °C). The catalyst was reduced in situ by placing 5–10 mg of $CuCr_2O_4$·CuO in the batch reactor, purging the reactor with H_2 to remove all oxygen, and starting a temperature ramp of 2.8, 2.6, and 2.4 °C/min to 240, 300, and 360 °C, respectively, for 1 h under a flow of 100 mL/min H_2 at atmospheric pressure and a 100-rpm stirring rate. The quantities 75 mL of *tert*-amyl alcohol solvent and 0.21 g of 5-methylfurfuryl alcohol were added to a 300-mL Parr batch reactor, which was subsequently purged by pressurizing/depressurizing it several times with hydrogen to remove oxygen from the headspace and any dissolved in the solvent. This mixture was then pumped into the reactor with hydrogen. The reactor was then pressurized to 220 psi H_2 and heated to 220 °C, at which point the first sample was taken, and the reactor repressurized to 500 psi H_2. Liquid samples were collected through a cooling coil immersed in an ice bath to prevent the reactant and product from vaporizing during sampling. Liquid samples were prepared by filtering through a 0.2-μm nylon syringe filter and analyzed using an Agilent Technologies 7890A gas chromatograph equipped with a HP-5MS column and an Agilent Technologies 5975C mass spectrometer to quantify the component concentrations.

3. Results

The diffractogram of the as-received copper chromite catalyst can be seen in Fig. 1. The characteristic diffractions of $CuCr_2O_4$ and CuO references 00-034-0424 and 00-048-1548, respectively, were present. The diffractograms of the reduced catalyst at the three reduction temperatures examined can be seen in Fig. 2. The sample reduced at 240 °C showed greatly diminished diffraction for $CuCr_2O_4$ at 35.25° and the formation of diffractions characteristic of the Cu^0 reference 00-004-0836. The broad diffraction at 36.5° has been attributed to the delafossite structure $CuCrO_2$ formed presumably from the reduction of $CuCr_2O_4$ spinel [32–35]. The sample reduced at 300 °C no longer showed diffraction peaks for $CuCr_2O_4$,

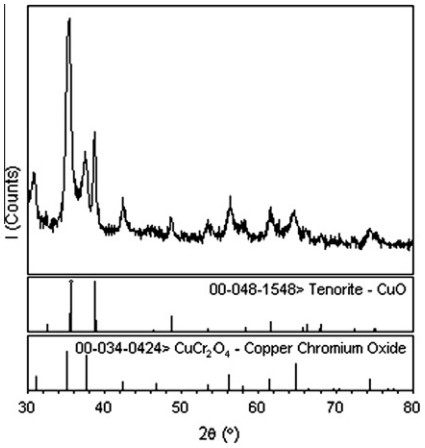

Fig. 1. Diffractogram of as-received copper chromite catalyst $CuCr_2O_4$·CuO and Cu:Cr = 1.

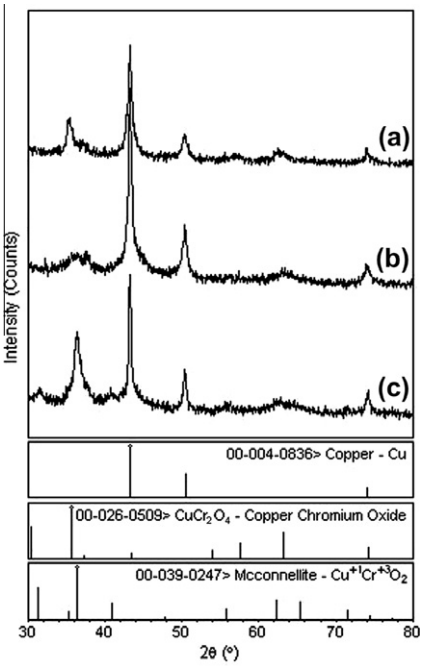

Fig. 2. Diffractogram of copper chromite catalyst reduced at: (a) 240 °C, (b) 300 °C, (c) 360 °C. Passivated in 1% O_2 at room temperature prior to analysis.

and only the diffractions for Cu^0 and $CuCrO_2$ were present. Similarly, the sample reduced at 360 °C revealed a diffraction pattern with contributions from only Cu^0 and $CuCrO_2$. The peak at 36.5° corresponding to $CuCrO_2$ became sharper and of a higher relative intensity than the sample reduced at 300 °C.

The reduction of the $CuCr_2O_4$·CuO starting material was also followed using H_2-TPD up to 600 °C, which can be seen in Fig. 3. The first reduction event had an onset at 145 °C and a maximum at 166 °C, which was followed by two smaller reduction events at 330 and 448 °C. The reduction at 166 °C was at least partially due to CuO reduction to Cu^0; however, the peak was not well resolved, and it was difficult to determine whether the two reduction events were convoluted. The reduction event at 330 °C could be characteristic of bulk reduction of $CuCr_2O_4$ to $CuCrO_2$ as described by Iimura et al. or of reduction of $CuCrO_2$ [32,36]. The reduction at 448 °C could be due to the complete reduction of the remaining mixed oxide structure to form Cu^0 and Cr_2O_3 [36].

Changing from bulk characterization to surface property characterization, physisorption and chemisorption data for $CuCr_2O_4$·CuO reduced at the three temperatures used in the study can be seen in

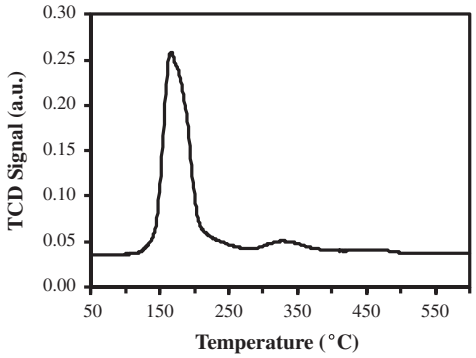

Fig. 3. H_2-TPR of copper chromite catalyst reduced with 10% H_2 in Ar at 5 °C/min observed by TCD.

Table 1. The reduction of $CuCr_2O_4$·CuO increased the surface area from the original 10.3 m^2/g to higher values with the reduced materials, which is consistent with other literature reports [12]. The amount of surface Cu^0 was determined using the N_2O titration method as described in Section 2. The material reduced at 240 °C gave 3.37 m^2/g of Cu^0, which accounted for approximately 20% of the catalyst surface, whereas reduction at 300 °C nearly doubled the surface concentration of Cu^0. The more severe reduction at 360 °C slightly reduced the metallic copper surface area, which was likely due to sintering of the surface metallic Cu. The irreversible CO chemisorption method, used to identify Cu^+ sites, revealed a trend similar to that with the Cu^0, but with larger changes. Reduction of $CuCr_2O_4$·CuO at 300 °C increased the Cu^+ by a factor of 2.6 relative to the material reduced at 240 °C, and the highest-temperature reduction nearly halved the amount of surface Cu^+ sites compared with that for of reduction at 300 °C. From these measurements, the surface concentration of the Cu^+ sites, which were assumed to irreversibly adsorb CO, was estimated to account for only about 1–3% of the surface area of the catalyst. The results suggested that significantly more Cu^0 was present on the surface of the reduced materials than Cu^+.

To examine surface acidity, NH_3-TPD was performed, and the results showed two distinct trends, as in Table 1. First, the total number of acid sites decreased significantly as the reduction temperature was increased. In particular, a large decline in acid site number was observed after the reduction at 360 °C. The second trend was that apparently stronger acid sites were present as the reduction conditions became more severe. The desorption maxima for NH_3 were 378, 424, and 454 °C after reduction at 240, 300, and 360 °C, respectively.

XPS and AES were both used to further evaluate the differences between surface and bulk properties observed by XRD and the chemisorption techniques, and an independent method to corroborate the trends measured for Cu^0 and Cu^+ in the chemisorption experiments. The XPS results for copper and chromium can be seen in Figs. 4 and 5, respectively, and were used to determine the possible oxidation states present near the surface for these species. The Cu2$p_{3/2}$ spectra of copper chromite reduced at any of the temperatures showed that no surface Cu^{2+} species existed after reduction due to the absence of satellite peaks associated with CuO and $CuCr_2O_4$ at BE of 943.1 and 942.2 eV, respectively [36–38]. This feature of the spectra allowed the correction of minor amounts of charging due to the oxide structure by shifting the remaining Cu^0 and Cu^+ peaks to 932.8 eV. XPS cannot be used to differentiate the peak at 932.8 eV between Cu^0 and Cu^+ species because they are separated by only 0.1 eV and neither would exhibit satellite peaks.

The two peaks shown in Fig. 5, which gives the XPS spectra for Cr, can be attributed to the Cr2$p_{3/2}$ and Cr2$p_{1/2}$ peaks of Cr^{3+} at 577 and 586 eV, respectively [37,39,40]. The presence of Cr^{6+}, which has a BE of approximately 580 eV, was not observed [37,39]. This result was consistent with the expectations that Cr^{6+} would not be formed under reducing conditions, and Cr^{3+} would only be present in the form of the $CuCr_2O_4$ spinel, the reduced spinel, or possibly a corundum structure of Cr_2O_3.

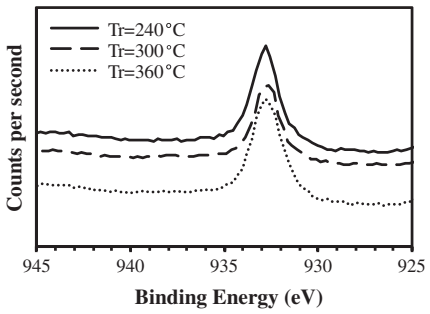

Fig. 4. XPS spectra of Cu2$p_{3/2}$ of copper chromite catalyst reduced at various temperatures.

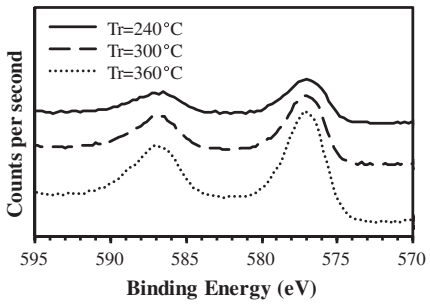

Fig. 5. XPS spectra of Cr2$p_{3/2}$ and Cr2$p_{1/2}$ of copper chromite catalyst reduced at various temperatures.

AES was used to deconvolute the contributions of Cu^0 and Cu^+ because the KE of their Auger electrons are separated by approximately 2 eV [36,37,41]. Fig. 6 shows the AES contributions of Cu^0 and Cu^+ at 918.3 and 916.0, respectively. From these data, it was possible to distinguish that the relative ratio of Cu^+:Cu^0 increased slightly when the reduction temperature was increased from 240 to 300 °C and decreased more significantly when the reduction temperature was further from 300 to 360 °C, which was consistent with the trend observed from the chemisorption experiments. These two contributions were fit using CasaXPS software to quantify the relative areas, and the results from this quantification are given in Table 2.

The specific activity of the catalysts, initial rate of reaction divided by catalyst BET surface area, can be seen in Table 1. The material that showed the highest specific activity was that reduced at 300 °C, which was consistent with that reported by Rao et al. in hydrogenation of furfural [12,13]. Only the C–O hydrogenolysis product, DMF, was observed in the reactor sample as the hydrogenation product, 2,5-dimethyltetrahydrofuran, was not observed by GC–MS/FID for the initial conversion levels of 20–30% that were used for evaluating the specific activities. Copper chromite catalysts

Table 1
Summary of characterization and reaction data for copper chromite reduced at 240, 300, and 360 °C.

Reduction T (°C)	BET (m^2/g)[a]	Cu^0 (m^2/m^2 BET)[b]	Cu^+ (m^2/BET m^2)[c]	NH_3 TPD (mmol/g)	NH_3-TPD T (°C)	Reaction rate (μmol/m^2/min)[d]
240	16.2	0.208	0.0119 ± 0.0017	0.300 ± 0.015	378 ± 3	52.7 ± 13.3
300	13.7	0.386	0.0311 ± 0.0044	0.232 ± 0.017	424 ± 2	108.4 ± 11.5
360	15.4	0.311	0.0159 ± 0.0021	0.057 ± 0.006	454 ± 4	87.8 ± 6.4

[a] Total surface area determined by N_2 BET method.
[b] Cu^0 determined by N_2O titration.
[c] Cu^+ determined by CO chemisorption.
[d] Reaction rate determined by rate of production of 2,5-dimethylfuran + 2,5-dimethyltetrahydrofuran.

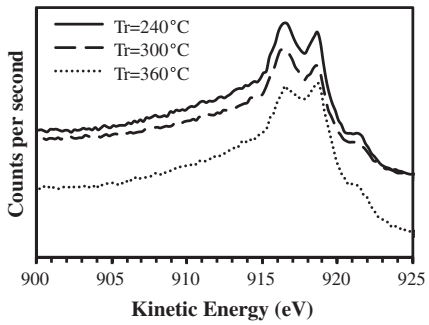

Fig. 6. AES spectra of Cu LMM of copper chromite reduced at various temperatures.

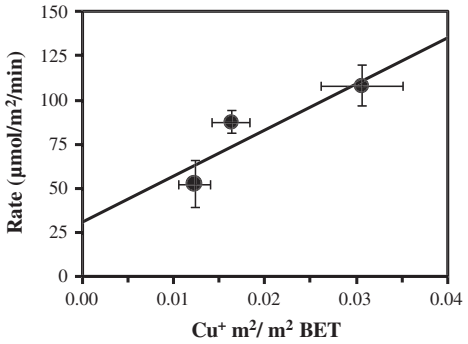

Fig. 8. Correlation between specific activity and surface concentration of Cu^+.

Table 2
Peak area of Cu^0 and Cu^+ in AES and comparison of the relative Cu^+:Cu^0 of AES and chemisorption results.

$T_{reduced}$ (°C)	AES Cu^+ (peak area)	AES Cu^0 (peak area)	AES Cu^+:Cu^0	Chemi Cu^+:Cu^0
240	16,854	20,340	0.83	0.059
300	16,031	15,363	1.04	0.079
360	13,560	21,057	0.64	0.052

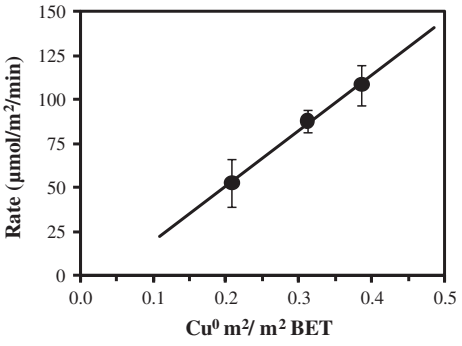

Fig. 7. Correlation between specific activity and surface concentration of Cu^0.

have been demonstrated to typically achieve selectivities exceeding 95% in hydrogenolysis to DMF. The overall carbon balances for the reaction systems were approximately 93% with the catalyst reduced at 240 °C, whereas the 300 and 360 °C catalysts gave mass balances of over 96%. As shown in Table 1, differences in surface areas of the materials alone were not enough to explain the trend in specific activity; therefore, it was apparent that modifying the surface concentrations of the copper species via different reduction treatments altered the resulting activity of the catalyst system.

In preliminary experiments, 1-butanol was used as the solvent, but it was found to give considerable dehydrogenation to butyraldehyde, and subsequent acetal formation was then observed. A tertiary alcohol, *tert*-amyl alcohol (2-methyl-2-butanol), was used to avoid dehydrogenation and the formation of activated hydrogen on the catalyst surface. It has been proposed that coupling reactions can affect and enhance catalytic performance or selectivities [20,21,23]. However, tertiary alcohols are more readily dehydrated than primary alcohols, and some minor formation of 2-methylbutene isomers was observed in the MS spectra. Furthermore, small amounts of products of etherification between 5-methylfurfuryl alcohol and 2-methylbutene were also observed in the MS spectra, but only accounted for approximately 2–5% of the carbon mass balance.

4. Discussion

The results from TPR, XRD, XPS, and chemisorption characterization can be used together to better understand the reduction behavior of the copper chromite catalyst. Based on the XRD results, the reduction at 240 °C did not completely eliminate the presence of the $CuCr_2O_4$ spinel species, but it did appear to be attenuated. The CuO was readily reduced to form Cu^0, as no Cu_2O was observed. Therefore, it could be concluded that the first TPR peak was a convoluted peak in which both the reduction of $CuCr_2O_4$ and CuO occurred. This convoluted peak also showed a slow return to the overall baseline, which might be consistent with the spinel being slowly and incompletely reduced, as indicated by XRD. The XPS results revealed that CuO and $CuCr_2O_4$ were completely reduced by 240 °C, as the surface was found to be comprised of only Cu^0 and Cu^+ copper species.

Following the reduction at 300 °C, the bulk reduction of $CuCr_2O_4$ was completed, as indicated by XRD. The XPS and AES results showed complete reduction of Cu^{2+} occurring by 240 °C, and the chemisorption and titration results showed increasing amounts of Cu^0 and Cu^+. This might be explained by a surface rearrangement in which more of these species became exposed or a partial decomposition of $CuCrO_2$, which would generate Cu^0 and Cr_2O_3. The latter explanation would seem to be most consistent with the onset of a reduction event near 300 °C, as indicated by TPR. This reduction scheme would be generally consistent with the study of Iimura et al. [36]; however, one point of distinction is that this study used $CuCr_2O_4$·CuO instead of just the spinel structure $CuCr_2O_4$.

Reduction at 360 °C significantly reduced the Cu^+ observed by CO chemisorption and would be consistent with the small reduction event that was seen at 330 °C with TPR. This event might have been due to partial decomposition of the $CuCrO_2$ structure, but it did not correspond to complete reduction, because the AES still showed the presence of some Cu^+. The loss of Cu^0 area could be explained by sintering copper into larger particles. The loss of Cu^0 and Cu^+ could also be explained by the partial decomposition of $CuCrO_2$ allowing Cr_2O_3 to begin to cover more of the catalyst surface, thereby blocking these species. The very small reduction event at approximately 450 °C could be the complete reduction of $CuCrO_2$, which would be consistent with the report of Iimura et al. [36].

The AES peak areas reported in Table 2 show the relative trends of Cu^+:Cu^0. A higher ratio Cu^+:Cu^0 was obtained by increasing the reduction temperature from 240 °C to 300 °C. Increasing the reduction temperature further to 360 °C reduced the ratio more dramatically, such that the ratio of Cu^+:Cu^0 was lower than at either 240 or 300 °C. When this was compared with the results of chemisorption, the same trend was observed. However, the values of Cu^+:Cu^0 as calculated from the AES spectra were considerably higher than the ratio determined by chemisorption. The relative enrichment

of Cu^0 on the surface, as determined by chemisorption, might be explained by coverage of the copper chromium oxide with a thin layer of Cu^0. Khasin et al. showed that Cu^0 particles were bound epitaxially to the oxide of a copper chromite spinel following the reduction at 320 °C [42]. As the information depth of AES extends beyond the first several monolayers to a depth of 3–10 nm, this higher level of Cu^+ observed by AES might be due to the method measuring more Cu^+ within the underlying oxide phase.

There was no clear correlation between the total number of acid sites or the strength of those acid sites and the activity, as no maximum in either of the acidity parameters was observed at 300 °C. Additionally, there is no clear correlation between the acidity and the quantified Cu^+ species. The amount of etherification product was a minimum for the catalyst reduced at 360 °C, which might have been correlated with the smaller amount of acid sites. To completely eliminate the dehydrogenation and dehydration solvent side reactions, it would be necessary to find an alternative solvent, but the side reactions with *tert*-amyl alcohol were sufficiently minor not to be expected to influence the hydrogenolysis results.

The primary goal of this work was to identify the copper species or species responsible for catalytic activity in the hydrogenolysis reaction. Two general hypotheses were explored by analyzing the experimental results. The first was that the catalyst had only one active site, Cu^0, by which H_2 was activated and the reactant was adsorbed through the hydroxyl group and cleaved. The other hypothesis was similar to the one proposed by Rao et al., which included a two-site mechanism in which the Cu^0 species activated hydrogen and the Cu^+ species adsorbed the carbonyl group—in this case, the hydroxyl group [12,13]. These hypotheses could be explored by examining the relationship between the specific activity and the surface concentration of the Cu^0 and Cu^+ species.

The correlation of measured specific activity with the surface concentration of Cu^0 can be seen in Fig. 7. As shown, there was a strong correlation between the activity and the Cu^0 site density on the catalyst. In comparison, the correlation in Fig. 8 between specific activity and Cu^+ was positive but weaker. It is important to note that these two correlations were based on the assumption that the other site did not play a role in the catalysis, since the Cu^0 and Cu^+ surface species both varied in such a way that their values were not completely decoupled. The correlation in Fig. 7 was consistent with the first hypothesis of only Cu^0 being involved as the active site. In contrast, the correlation presented in Fig. 8 was not consistent with the hypothesis of a two-site mechanism. However, it should be noted that approximately 10–30 times more Cu^0 was present on the surface than active Cu^+ species. Therefore, it would be plausible that under such disproportionate conditions the activity could be limited by adsorption onto Cu^+, thereby providing a strong correlation even while upholding a two-site mechanism. However, there should not have been such a strong Cu^0 correlation with activity if this had been the case. The correlation of Cu^0 with the activity also had an intercept that was close to zero, which would be consistent with the expected limit that as the number of active sites approached zero, the activity would also approach zero. This zero intercept was not seen for the Cu^+ correlation comparison. These results suggested that the Cu^0 site density was responsible for catalytic activity, which could be explained by either Cu^0 as the sole active site or a two-site mechanism in which the activation or activation and migration of hydrogen from Cu^0 sites to a site adjacent to the hydroxyl adsorption site was the rate-limiting step in the catalytic cycle. However, these results cannot rule out the role of Cu^+ in a two-site mechanism. Based on pseudo-Henry's-law constants for hydrogen in 1-butanol, the possibility that the solubility of hydrogen in *tert*-amyl alcohol could be the cause of a hydrogen deficient catalyst did not seem to be significant [43].

5. Conclusions

Copper chromite catalysts were extensively characterized and tested for catalytic activity in the C–O hydrogenolysis of 5-methylfurfuryl alcohol to DMF. XPS and AES quantifying the amounts of surface Cu^0 and Cu^+ were used to corroborate the chemisorption results and showed similar trends in the relative amounts of these two species upon various reduction treatments. TPR, in conjunction with other characterization results, was used to determine that the largest reduction event occurred at 166 °C, which is the convolution of CuO and $CuCr_2O_4$ reductions. Subsequent reduction events could be explained by a partial reduction of the proposed Cu^+ species, $CuCrO_2$, followed by a complete reduction at higher temperatures. It was also found that the reduction temperature affected the specific activity of the catalyst, which was caused by a change in the surface concentration of active species characterized as Cu^0 and Cu^+. Reduction at 300 °C coincided with the highest activity and the highest concentrations of Cu^0 and Cu^+ sites. Examining the relative correlations between activity and Cu^0 and Cu^+ site densities, suggested that Cu^0 was primarily responsible for the activity of the catalyst; however, the role of Cu^+ cannot be ruled out. Cu^0 could be the sole active site or, in the case of a two-site mechanism, would need to be the rate-limiting active site. Further studies would be necessary to fully and definitively differentiate these two possibilities.

Acknowledgments

This work was supported by National Science Foundation PIRE (OISE 0730227) and ERC (EEC-0813570). We would like to acknowledge the contribution of Stephanie Kühl in performing and assisting N_2O titration measurements under the direction of Dr. Malte Behrens and Professor Robert Schlögl of the Fritz Haber Institute AC Department. We would also like to acknowledge James Anderegg for operating the XPS/AES at Ames Lab and Professor Pat Thiel at ISU for XPS/AES data analysis discussions.

References

[1] S. Crossley, J. Faria, M. Shen, D.E. Resasco, Science 327 (2010) 68.
[2] Y. Roman-Leshkov, C.J. Barrett, Z.Y. Liu, J.A. Dumesic, Nature 447 (2007) 982.
[3] B.L. Scallet, J.H. Gardner, J. Am. Chem. Soc. 67 (1945) 1934.
[4] C.J. Moye, Z.S. Krzeminski, Aust. J. Chem. 16 (1963) 258.
[5] K. Sipila, E. Kuoppala, L. Fagernas, A. Oasmaa, Biomass Bioenergy 14 (1998) 103.
[6] S. Sitthisa, T. Sooknoi, Y.G. Ma, P.B. Balbuena, D.E. Resasco, J. Catal. 277 (2011) 1.
[7] M.S. Borts, N.D. Gilchenok, V.M. Ignatev, G.S. Gurevich, J. Appl. Chem. USSR 59 (1986) 114.
[8] J.G.M. Bremner, R.K.F. Keeys, J. Chem. Soc. (1947) 1068.
[9] R.M. Lukes, C.L. Wilson, J. Am. Chem. Soc. 73 (1951) 4790.
[10] B.M. Nagaraja, A.H. Padmasri, B.D. Raju, K.S.R. Rao, J. Mol. Catal. A: Chem. 265 (2007) 90.
[11] M. Pramottana, P. Praserthdam, B. Ngamsom, J. Chin. Inst. Chem. Eng. 33 (2002) 477.
[12] R. Rao, A. Dandekar, R.T.K. Baker, M.A. Vannice, J. Catal. 171 (1997) 406.
[13] R.S. Rao, R.T.K. Baker, M.A. Vannice, Catal. Lett. 60 (1999) 51.
[14] G. Seo, H. Chon, J. Catal. 67 (1981) 424.
[15] E. Soner, T. Dogu, Y. Yorulmaz, Arab. J. Sci. Eng. 21 (1996) 321.
[16] J. Wu, Y.M. Shen, C.H. Liu, H.B. Wang, C. Geng, Z.X. Zhang, Catal. Commun. 6 (2005) 633.
[17] B.M. Reddy, G.K. Reddy, K.N. Rao, A. Khan, I. Ganesh, J. Mol. Catal. A: Chem. 265 (2007) 276.
[18] L.W. Burnette, I.B. Johns, R.F. Holdren, R.M. Hixon, Ind. Eng. Chem. 40 (1948) 502.
[19] D.G. Manly, A.P. Dunlop, J. Org. Chem. 23 (1958) 1093.
[20] H.Y. Zheng, J. Yang, Y.L. Zhu, G.W. Zhao, React. Kinet. Catal. Lett. 82 (2004) 263.
[21] H.Y. Zheng, Y.L. Zhu, L. Huang, Z.Y. Zeng, H.J. Wan, Y.W. Li, Catal. Commun. 9 (2008) 342.
[22] H.Y. Zheng, Y.L. Zhu, B.T. Teng, Z.Q. Bai, C.H. Zhang, H.W. Xiang, Y.W. Li, J. Mol. Catal. A: Chem. 246 (2006) 18.
[23] Y.L. Zhu, H.W. Xiang, Y.W. Li, H.J. Jiao, G.S. Wu, B. Zhong, G.Q. Guo, New J. Chem. 27 (2003) 208.
[24] E. Furimsky, Appl. Catal. A: Gen. 199 (2000) 147.

[25] M.J. Girgis, B.C. Gates, Ind. Eng. Chem. Res. 30 (1991) 2021.
[26] J. Zakzeski, P.C.A. Bruijnincx, A.L. Jongerius, B.M. Weckhuysen, Chem. Rev. 110 (2010) 3552.
[27] J.B. Hansen, P.E.H. Nielsen, in: G. Ertl, H. Knozinger, F. Schuth, J. Weitkamp (Eds.), Handbook of Heterogeneous Catalysis, Wiley-VCH Verlag GmbH & Co. KGaA, Weinheim, 2008, p. 2920.
[28] H.E. Hoydonckx, W.M. Van Rhijn, W. Van Rhijn, D.E. De Vos, P.A. Jacobs, in: Ullmann's Encyclopedia of Industrial Chemistry, Wiley-CVH Verlag GmbH & Co. KGaA, 2007.
[29] R.M. Dell, F.S. Stone, P.F. Tiley, Trans. Faraday Soc. 49 (1953) 201.
[30] J.W. Evans, M.S. Wainwright, A.J. Bridgewater, D.J. Young, Appl. Catal. 7 (1983) 75.
[31] J.J. Scholten, Konvalin Ja, Trans. Faraday Soc. 65 (1969) 2465.
[32] R.B.C. Pillai, Catal. Lett. 26 (1994) 365.
[33] S.P. Tonner, M.S. Wainwright, D.L. Trimm, N.W. Cant, Appl. Catal. 11 (1984) 93.
[34] G.L. Castiglioni, A. Vaccari, G. Fierro, M. Inversi, M.L. Jacono, G. Minelli, I. Pettiti, P. Porta, M. Gazzano, Appl. Catal. A: Gen. 123 (1995) 123.
[35] J.R. Monnier, M.J. Hanrahan, G. Apai, J. Catal. 92 (1985) 119.
[36] A. Iimura, Y. Inoue, I. Yasumori, Bull. Chem. Soc. Jpn. 56 (1983) 2203.
[37] F.M. Capece, V. Dicastro, C. Furlani, G. Mattogno, C. Fragale, M. Gargano, M. Rossi, J. Electron Spectrosc. 27 (1982) 119.
[38] G.R. Apai, J.R. Monnier, M.J. Hanrahan, J. Chem. Soc. Chem. Commun. (1984) 212.
[39] J.M. Camposmartin, A. Guerreroruiz, J.L.G. Fierro, J. Catal. 156 (1995) 208.
[40] J. Christopher, C.S. Swamy, J. Mater. Sci. 27 (1992) 1353.
[41] G. Apai, J.R. Monnier, M.J. Hanrahan, Appl. Surf. Sci. 19 (1984) 307.
[42] A.A. Khasin, T.M. Yur'eva, L.M. Plyasova, G.N. Kustova, H. Jobic, A. Ivanov, Y.A. Chesalov, V.I. Zaikovskii, A.V. Khasin, L.P. Davydova, V.N. Parmon, Russ. J. Gen. Chem. 78 (2008) 2203.
[43] J.V.H. d'Angelo, A.Z. Francesconi, J. Chem. Eng. Data 46 (2001) 671.